

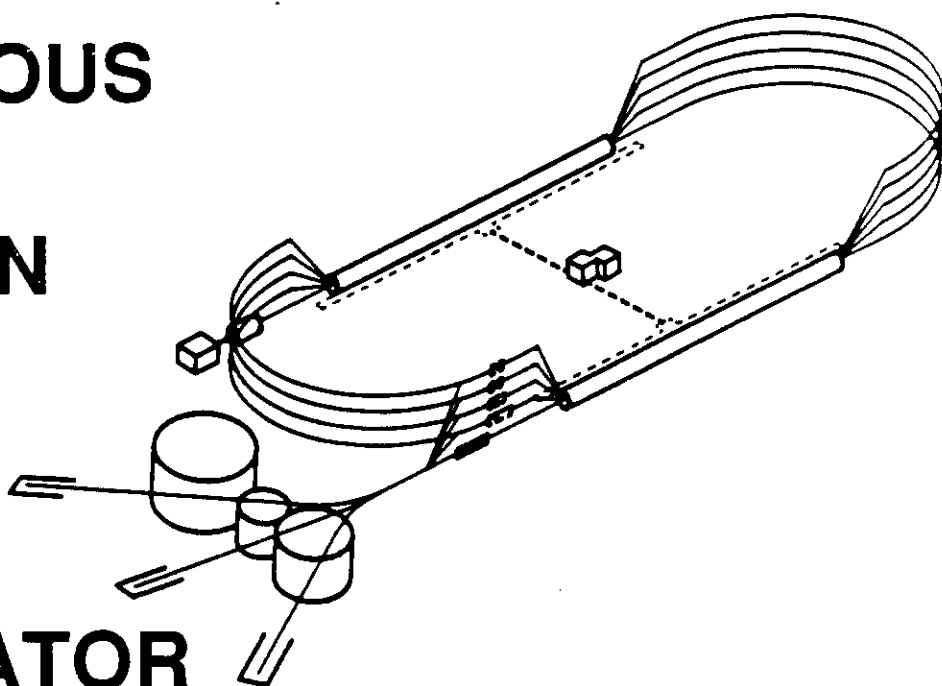
# Light Quark Baryons

Volker Burkert  
Continuous Electron Beam Accelerator Facility  
Newport News, VA 23606

Invited talk presented at the Rheinfels Workshop 1990 Hadron Mass Spectrum,  
St. Goar, Germany, September 3 - 6, 1990

# C E B A F

CONTINUOUS  
ELECTRON  
BEAM  
ACCELERATOR  
FACILITY



**SURA** *Southeastern Universities Research Association*

**CEBAF**  
The Continuous Electron Beam Accelerator Facility  
Newport News, Virginia

# LIGHT QUARK BARYONS

Volker D. Burkert

Continuous Electron Beam Accelerator Facility,  
12000 Jefferson Avenue, Newport News, Virginia 23606, USA.

The status of hadronic and electromagnetic excitation of light quark (u, d) baryon states is reviewed and confronted with results of calculations within the framework of microscopic models of the baryon structure and the photon - baryon coupling. Prospects for a qualitative improvement of our knowledge in this sector using photon and electron beams at the new, intermediate energy cw electron machines are discussed.

## 1. INTRODUCTION

Understanding the structure of hadrons in terms of the fundamental interaction of the constituent quarks and gluons is one of the challenges in intermediate energy physics. The study of hadron spectroscopy using hadronic probes has taught us a great deal about the underlying symmetries and interactions. In this talk I focus on the electromagnetic transition between baryon states, a sector that has, to some degree, been neglected in the past, largely because of the low rates associated with electromagnetic interactions. This made it difficult to achieve the precision needed for a detailed analysis of the entire resonance region in terms of the fundamental photocoupling amplitudes. With the construction of CW electron accelerators in the GeV and multi-GeV region, this situation is changing in a significant way<sup>1</sup>. It may therefore be appropriate to review, in some detail, the status of this field. Photo- and electroexcitation of baryon resonances yield information about the  $\gamma_b NN^*$  vertex as a function of the four-momentum transfer  $Q^2$ . This allows tests of theoretical models describing the electromagnetic coupling of photons to baryons, and the probing of the structure of baryons and their excited states.

The interaction of the baryon constituents, quarks and gluons, is generally perceived to be described by QCD, the theory of strong interactions. However, solutions of this theory in the non-perturbative domain are extremely difficult to achieve. The lattice gauge theory offers the best hope for exact calculations, but results seem to be far in the future. Thus, models will continue to play an important role. Microscopic models, such as dynamical quark models, bag models, Skyrme models, and QCD sum rules, relate the internal baryon structure to the strong interaction of the confined constituents.

Probing baryons with photons and electrons will give us insight into this fundamental interaction.

This is the main thrust of experiments using the electromagnetic probe. Before reviewing the experimental status of electromagnetic transitions of baryon resonances, I briefly summarize the status of light quark baryon spectroscopy.

## 2. SUMMARY OF LIGHT QUARK BARYON SPECTROSCOPY

In course of the past decade, very little has happened in experimental light quark baryon spectroscopy. The field has been left by the particle physics community in a deplorable state. The 1990 edition of the Review of Particle Properties<sup>2</sup> (RPP) lists 23 established  $N^*$  or  $\Delta$  states, and about as many candidate states with insufficient experimental evidence. However, this is only a small fraction of the states predicted by QCD inspired quark models. Most of this information is the result of partial wave analyses of pion-nucleon scattering measurements  $\pi N \rightarrow \pi N$ . The methods used, the results of the analyses, and remaining problems have been discussed in recent reviews<sup>3</sup>.

The non-relativistic quark model<sup>4</sup> and its relativistic extension<sup>5</sup> allows the association of all established states with a level in the quark model. The ground states and all states associated with the  $[70, 1^-]_1$  super multiplet have been observed experimentally. However, several of the  $N=2$  states, and most of the  $N=3$  and  $N=4$  states have not been seen in  $\pi N \rightarrow \pi N$  reactions. Figure 2.1 and Figure 2.2 summarize the experimental situation for the  $N=2$  and  $N=3$  super multiplets. After an overall adjustments of the center-of-mass excitation energies, the predicted levels for most of the states are in fair agreement with the measured masses. There are few exceptions, where the discrepancies are significantly beyond the experimental errors. The  $D_{35}(1930)$  is such

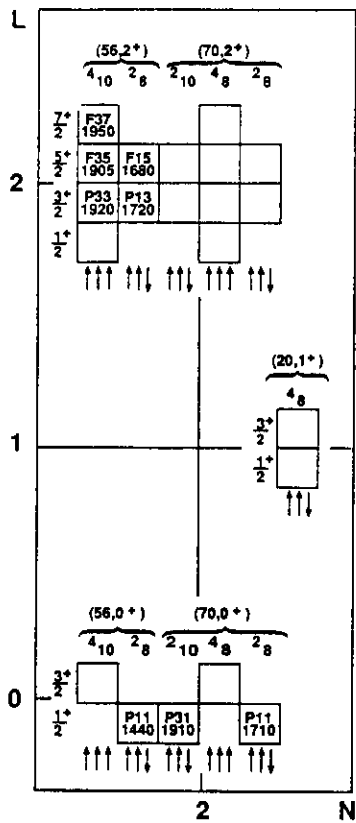


Figure 2.1 Experimental status of the  $N=2$  quark model states. The graph is from Ref.[6] (slightly modified)

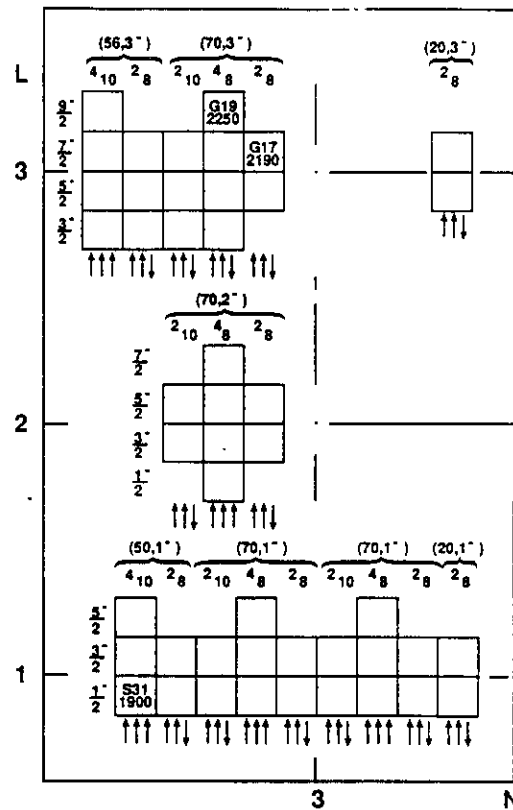


Figure 2.2 Experimental status of the  $N=3$  quark model states. The graph is from Ref.[6] (slightly modified)

State	Mass (MeV)	Widths (MeV)
$P_{11}(1440)$	1400-1480	120-350
$P_{13}(1720)$	1690-1800	125-250
$D_{33}(1700)$	1630-1740	190-300
$S_{31}(1900)$	1850-2000	130-300
$P_{33}(1920)$	1860-2060	190-300

a case. The experimental mass is 1890 to 1960 MeV. The model of Forsyth and Cutkosky<sup>7</sup> predicts a  $D_{35}$  state at 2131 MeV, and the model of Capstick and Isgur<sup>5</sup> at 2030 MeV. The fact that there is only fair agreement between experimental resonance masses and

masses predicted in quark model calculations is not necessarily alarming. It is well known that dynamic effects, such as pion re-scattering may contribute to shifts in resonance masses. These effects have not been taken into account in current quark model calculations.

An intriguing observation is the apparent clustering of resonance masses. Many states appear to cluster in certain mass regions. For example, six  $N^*$  states and two  $\Delta$  states cluster in a mass range from 1620 to 1720 MeV. There are another six  $\Delta$  states with masses from 1900 to 1950 MeV. Is this clustering accidental, or is there a mechanism at work that pulls these states together? A possible explanation is presented in the talk of D. Bugg<sup>9</sup>. Experimental uncertainties in the widths of many states are large. In the case of the  $P_{11}(1440)$ , the uncertainty is nearly a factor of 3. Table 2.1 shows experimental masses and widths for some states, with their uncertainties as listed in the RPP. The  $P_{11}(1440)$  is listed as a single well established resonance. This conclusion is based upon the Karlsruhe-Helsinki<sup>10</sup> and the CMU-LBL<sup>11</sup> partial wave analyses. The signif-

State	$\pi N$	$\eta N$	$N\pi\pi$
$P_{11}(1710)$	10-20	$\sim 25$	$\leq 50$
$P_{13}(1720)$	10-20	$\sim 3.5$	$\leq 75$
$G_{17}(2190)$	$\sim 14$	$\sim 3$	?
$H_{19}(2220)$	$\sim 18$	$\sim 0.5$	?
$G_{19}(2250)$	$\sim 10$	$\sim 2$	?
$I_{11,1}(2600)$	5	$\sim 2$	?
$P_{31}(1910)$	15-25	-	$\leq 75$
$P_{33}(1920)$	15-20	-	?
$D_{35}(1950)$	5-15	-	not seen
$F_{37}(1710)$	35-45	-	$\leq 40$
$H_{3,11}(2420)$	5-15	-	?

icantly different values found for the width of this state in the two analyses is disturbing. Clearly, the analysis of this energy region is complicated due to the opening up of the  $\pi\Delta(1232)$  channel. In fact, Blankleider and Walker<sup>12</sup> have demonstrated that coupling to the  $\pi\Delta$  by itself can generate resonance like behaviour. In a more recent analysis by the VPI group<sup>13</sup> which included new of  $\pi N$  data in the energy region of the  $P_{11}(1440)$ , two poles were found in the complex energy plane, at (1359, -100i) and (1410, -80i) MeV. This result let to speculations about a possible splitting of the  $P_{11}$  into two states. Arguments have been presented<sup>14</sup> that such a double pole might just be what is expected from single resonances in the presence of open inelastic channels. While there is no conclusive evidence towards either one of these interpretations, recent  $\pi N \rightarrow \pi N$  data from LAMPF and Leningrad<sup>15</sup> in the energy regime of the  $P_{11}$  may afford a new analysis of the K-H or CMU-LBL type to shed more light on this problem.

### 2.1 Missing Baryons States

Koniuk and Isgur<sup>16</sup> have suggested that the problem of the missing states may be related to the lack of data in the inelastic channels. They predict most of the missing states decouple from the  $\pi N$  channel. The  $\pi N \rightarrow \pi N$  process becomes rather ineffective in this case. Many of the N=2 and N=3 states are predicted

to couple strongly to  $\Delta\pi$  and  $\rho N$ . If the  $\pi N$  channel does not totally decouple from the resonance, the process  $\pi N \rightarrow \pi\pi N$  may offer a better chance for detecting these states. Analyzing this channel in bubble chamber data, Manley<sup>17</sup> found evidence for one of the predicted states, a  $F_{35}$  with a mass around 2000 MeV. In case the decoupling from the  $\pi N$  channel is nearly complete, electromagnetic transitions may be the only way to search for these states. Obviously, our picture of baryon structure could change dramatically if these states did not exist. An extensive search for at least some of these states is urgent.

Inelastic channels are not well determined experimentally, due to the lack of sufficiently detailed data in the  $\pi N \rightarrow \pi\pi N$ ,  $\pi N \rightarrow \pi\pi\pi N$ , and  $\pi N \rightarrow \eta N$  channels (table 2.2). The lack of knowledge of these fundamental resonance properties has serious consequences regarding systematic uncertainties in the extraction of photocoupling amplitudes, where properties of the hadronic vertex are needed as input.

### 3. ELECTROMAGNETIC TRANSITIONS

The  $\gamma_0 NN^*$  vertex for the transition into a specific state is described by three (two for J=1/2 states) amplitudes,  $A_{1/2}(Q^2)$ ,  $A_{3/2}(Q^2)$ ,  $S_{1/2}(Q^2)$ , where A and S refer to the transverse and scalar coupling, respectively, and the subscripts refer to the total helicity of the  $\gamma_0 N$  system. Spin and isospin have to be extracted by measuring the angular distribution in different isospin channels. Many of the lower lying resonances ( $W \leq 1.8\text{GeV}$ ) decay dominantly into the  $N\pi$  or  $N\eta$  channel. Experiments have therefore concentrated on single  $\pi$  and  $\eta$  production. In the following section the current experimental situation is reviewed.

#### 3.1 Radiative Transitions with $\Delta L_{3Q} = 0$ .

The photo- and electroexcitation of the  $\Delta(1232)$  is predominantly mediated by a magnetic dipole transition  $M_{1+}$  corresponding to  $A_{1/2} = (1/\sqrt{3})A_{3/2}$ . In terms of the most naive, SU(6) symmetric quark models the transition is explained by a spin flip of one of the valence quarks in the nucleon ground state. In more elaborate, QCD based models the electric  $E_{1+}$  and scalar  $S_{1+}$  quadrupole contributions are predicted to be small but non-zero, corresponding to non spherical  $\Delta L_{3Q} = 2$  components. Table 3.1 shows results of model calculations for the ratio  $E_{1+}/M_{1+}$ .

Current data<sup>1</sup> are not precise enough to discriminate between most of the models. A possible exception is the Skyrme model which appears to be ruled out by the  $Q^2 = 0$  data. The data allow for a range  $E_{1+}/M_{1+} = 0$  to  $-1.5\%$  at  $Q^2 = 0$ . At high  $Q^2$  the ratio

Table 3.1 $E_{1+}/M_{1+}$ [%] for $\gamma_p N \Delta(1232)$			
Model	$Q^2 = 0$	$Q^2 < 3\text{GeV}^2$	$Q^2 \rightarrow \infty$
NRQM <sup>16,18</sup>	-0.7	-0.7 to -5.	
RQM <sup>16</sup>	-1.4	-1.4 to -5.	
MIT Bag <sup>19</sup>	0.		
Chiral Bag <sup>20,21</sup>	-0.9 to -1.8		
Skyrme <sup>22,23</sup>	-2.5 to -5.0		
pQCD <sup>24</sup>			+100.

cannot remain small, since perturbative QCD requires  $E_{1+}/M_{1+} \rightarrow +1$  at  $Q^2 \rightarrow \infty$ . Precise measurements of the  $Q^2$  dependence are obviously of great importance for the development of realistic models of the nucleon.

Electromagnetic excitation of the Roper resonance  $P_{11}(1440)$  is of particular interest. The QCD inspired non-relativistic quark model has difficulties in describing its radiative decay width. This discrepancy has raised questions<sup>25</sup> about the nature of the  $P_{11}(1440)$ . The SU(6) classification of the  $P_{11}(1440)$  is that of a  $[56, 0^+]_2$  state. Precise data on photo- and electroexcitation of the Roper can help reveal the true nature of this state. The non-relativistic quark model predicts for the neutron/proton ratio:  $A_{1/2}^n/A_{1/2}^p = -2/3$ , related to the magnetic  $M_{1-}$  transition. In chiral bag model calculations<sup>21</sup> this ratio is closer to -1 at  $Q^2 = 0$ , because of contributions from the pion cloud. With increasing  $Q^2$ , however, the role of the pion cloud should be diminished, and the quark composition is expected to dominate its properties at higher  $Q^2$ . An interesting consequence of the  $N = 2$  assignment of the  $P_{11}(1440)$  is its predicted dominance over the  $\Delta(1232)$  at high  $Q^2$ . The NRQM predicts:

$$\frac{A_{1/2}(P_{11}(1440))}{A_{1/2}(\Delta(1232))} \propto \bar{Q}^2.$$

The data are shown in Figure 3.1. The value -2/3 is clearly preferred for the neutron/proton ratio, however, a value closer to -1 is not ruled out. The  $Q^2$  dependence is virtually unknown. An analysis<sup>26</sup> of older DESY and NINA data at  $Q^2 = 1\text{GeV}^2$  suggests a zero crossing of the  $A_{1/2}$  amplitude at small  $Q^2$ . None of the explicit

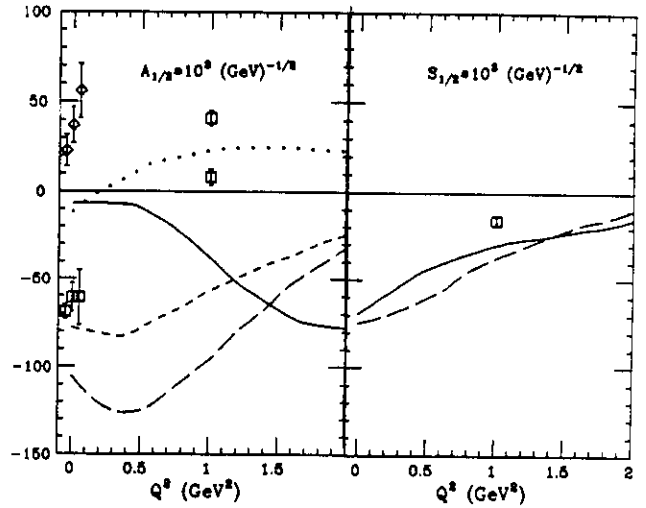


Figure 3.1 Transverse (left) and scalar (right) photo-coupling amplitudes of the Roper  $P_{11}(1440)$  for proton (open squares) and neutron targets. Calculations for protons by Foster and Hughes<sup>25</sup> (dots); Warns et al.<sup>18</sup> (NRQM: long dashes, RQM: solid); Li and Close<sup>27</sup> (short dashes).

quark models comes even near to describing the  $Q^2$  behaviour suggested by the  $Q^2 = 0$  and  $Q^2 = 1.0\text{GeV}^2$  data. Relativistic corrections give uncomfortably large effects, which spells some doubts about the validity of the ( $v/c$ ) expansion in this particular case. Predictions for the longitudinal (scalar) coupling are much less sensitive to relativistic corrections. In some quark model calculations<sup>16</sup> the transition to the  $P_{11}(1440)$  is predicted to exhibit an exceptionally strong longitudinal coupling. The predictions are in fair agreement with the  $Q^2 = 1\text{GeV}^2$  analysis (Figure 3.1). Clearly, more precise and more complete data are needed for more definite tests of the above mentioned predictions.

### 3.2 Radiative Transitions between the $[56, 0^+]_0$ and the $[70, 1^-]_1$ Multiplets

Of the seven  $S=0$  states associated with the  $[70, 1^-]_1$  multiplet only the  $D_{13}(1520)$  and the  $S_{11}(1535)$  have been studied with electromagnetic probes, in some detail.

#### 3.2.1 The $\gamma_p p \rightarrow S_{11}(1535)$ Transition

The  $S_{11}(1535)$  is characterized by a large branching ratio into the  $\eta N$  channel ( $\approx 50\%$ ). Since the nearby  $D_{13}(1520)$  state has a very small decay width into  $\eta N$  the  $S_{11}(1535)$  can be separated off in a rather straight forward manner. Electroproduction results indicate a slow falloff with  $Q^2$  (Figure 3.2). Up until recently,

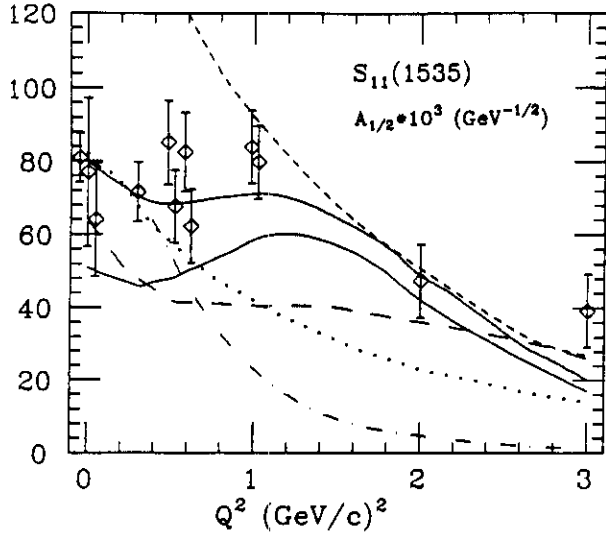


Figure 3.2 Transverse photocoupling amplitude  $A_{1/2}$  for the transition  $\gamma_{vp}S_{11}(1535)$ . Model calculations by Li and Close<sup>27</sup> (short dashes), Warns et al.<sup>8</sup> (solid lines, for different confinement potentials), Foster and Hughes<sup>28</sup> (dots), Konen and Weber<sup>29</sup> (long dashes), Forsyth and Babcock<sup>30</sup> (dashed-dotted).

this behaviour could not be explained within the framework of quark models. However, recent extensions of the model to include relativistic effects have been quite successful in reproducing this particular behaviour. It is interesting to note that within the framework of a specific model, the absolute normalization appears to be sensitive to the parameterization of the confinement potential. This lends confidence to the idea that by carefully studying many resonance transitions, a great deal can be learned about the confinement potential.

### 3.2.2 The $\gamma_{vp} \rightarrow D_{13}(1520)$ Transition

At  $Q^2 = 0$ , the  $D_{13}(1520)$  is predominantly excited by  $A_{3/2}$  transitions. With increasing  $Q^2$ ,  $A_{1/2}$  becomes the dominant contribution. This is demonstrated by displaying the helicity asymmetry

$$A_{\frac{1}{2},\frac{3}{2}} = \frac{A_{1/2}^2 - A_{3/2}^2}{A_{1/2}^2 + A_{3/2}^2}.$$

A summary of the data is presented in Figure 3.3. It is worth noting that effects due to the radial wave function tend to drop out in this quantity. The helicity asymmetry is therefore sensitive to the photon-quark dynamics. The noted helicity switch is qualitatively in accordance with quark model predictions<sup>31</sup>, as well as with expectations from helicity conservation in perturbative QCD at high  $Q^2$ . However, it is the details, of how, and at what

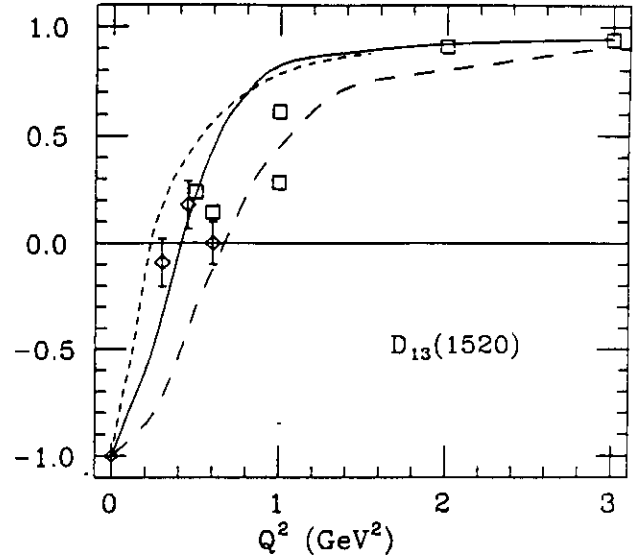


Figure 3.3 Helicity asymmetry of the  $\gamma_{vp}D_{13}(1520)$  transition. Quark-model calculations by Ono<sup>50</sup> (long dashes), Copley<sup>51</sup> (short dashes), Li and Close<sup>27</sup> (NRQM solid)

$Q^2$  this transition occurs that will provide us with more insight into the internal dynamics of the nucleon<sup>25</sup>.

### 3.2.3. Test of the Single Quark Transition Model

Within the framework of single quark transitions in  $SU(6)_W$  symmetric models, radiative transitions between the  $[56, 0^+]_0$  and the  $[70, 1^-]_1$  multiplet are described by 3 amplitudes<sup>32</sup>, called A, B, and C. These are related to the quark orbit flip current, the quark spin flip current, and the combined spin flip and orbit flip current with  $\Delta L_z = 1$ , respectively. Radiative transitions between all states belonging to these multiplets can be expressed in terms of linear combinations of these amplitudes.

Knowledge of the  $A_{1/2}$ ,  $A_{3/2}$  amplitudes for the  $S_{11}(1535)$  and the  $D_{13}(1520)$  states allow the determination of the A, B, C single quark transition amplitudes. These can then be used to predict transition amplitudes for other states. Recent calculations in a relativized quark model<sup>18</sup> predict deviations from the SQTm at the 20% level. Unfortunately, information from other states is limited to proton targets and is of poor quality. Current experimental information of the  $S_{11}(1650)$ ,  $S_{31}(1620)$ , and  $D_{33}(1700)$  is summarized in Figure 3.4. The data are not in disagreement with the SQTm predictions, however, they are not accurate enough to test deviations from the SQTm at the predicted level.

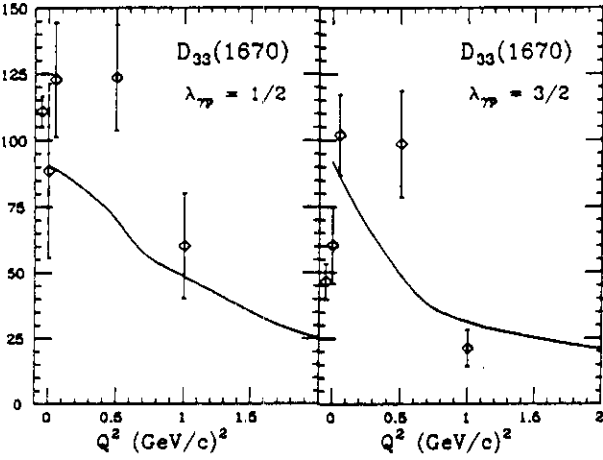
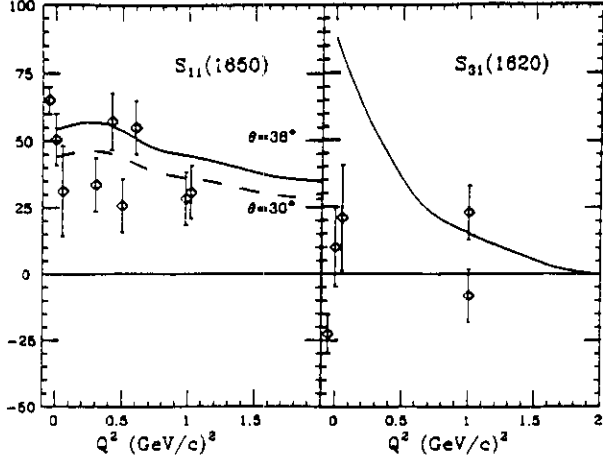


Figure 3.4 Transverse photocoupling amplitudes for the  $S_{11}(1650)$ ,  $S_{31}(1620)$ , and  $D_{33}(1700)$  states. The curves represent SQT M predictions using  $S_{11}(1535)$  and  $D_{13}(1520)$  data and the algebraic relations of Hey and Weyers<sup>32</sup>.  $\Theta$  is the mixing angle between the  $[^48]$  and  $[^28]$  states in  $[70, 1^-]$ .

### 3.2.4 Quark Multipoles for $\gamma_e + [56, 0^+]_0 \rightarrow [70, 1^-]_1$

The single quark transition amplitudes can be expressed in terms of quark electric and quark magnetic multipoles<sup>33</sup>,  $e_\lambda^{LL}$ ,  $m_\lambda^{LL}$ ,  $m_\lambda^{L, L+1}$ , the first one being related to the quark orbit flip, the latter ones to the quark spin flip, and the quark spin-orbit flip amplitudes. For the transition  $[56, 0^+]_0 \rightarrow [70, 1^-]_1$  one obtains<sup>34</sup> (in units of  $[\mu b GeV]^{1/2}$ )

$$A = 8.88e_1^{11}$$

$$1/2(B - C) = -6.31m_1^{11}$$

$$1/2(B + C) = +6.31m_1^{12}$$

More direct information about the photon quark dynamics can be obtained by factoring out an explicit dipole formfactor dependence

$$F(\bar{Q}_{evf}^2) = \frac{1}{(1 + \bar{Q}_{evf}^2/0.71)^2},$$

where the 3-momentum is evaluated in the equal velocity frame ( $\vec{v}_N = -\vec{v}_N$ ) to minimize relativistic effects. The only justification for such a choice is the fact that it describes the  $Q^2$  dependence of the elastic formfactor (note that  $\bar{Q}_{evf}^2 = Q^2$  for elastic scattering). Using this expression, reduced quark multipoles can be defined as:

$$e_1^{11} = \bar{e}_1^{11} F(\bar{Q}_{evf}^2); \quad m_1^{11} = \bar{m}_1^{11} F(\bar{Q}_{evf}^2);$$

$$m_1^{12} = \bar{m}_1^{12} F(\bar{Q}_{evf}^2)$$

$$e_1^{22} = \bar{e}_1^{22} |\bar{Q}_{evf}| F(\bar{Q}_{evf}^2); \quad m_1^{22} = \bar{m}_1^{22} |\bar{Q}_{evf}| F(\bar{Q}_{evf}^2);$$

$$m_1^{23} = \bar{m}_1^{23} |\bar{Q}_{evf}| F(\bar{Q}_{evf}^2)$$

The results for the  $[70, 1^-]_1$  multiplet are displayed in Figure 3.5. The reduced multipoles  $\bar{e}_1^{11}$ , and  $\bar{m}_1^{11}$  exhibit a very simple  $\bar{Q}_{evf}^2$  dependence.  $\bar{e}_1^{11}$  is independent of  $\bar{Q}_{evf}^2$ , and  $\bar{m}_1^{11}$  rises linearly with  $\bar{Q}_{evf}^2$ . At small  $\bar{Q}_{evf}^2$ ,  $\bar{m}_1^{12}$  has nearly the same slope as  $\bar{m}_1^{11}$ . This indicates that the reduced spin orbit term  $\bar{C}$  is approximately constant at  $\bar{Q}_{evf}^2 < 1.5 GeV^2$ . The simplicity of the  $\bar{Q}_{evf}^2$  dependence calls for a simple explanation. To my knowledge there has not been any theoretical effort to describe this behaviour of the quark multipoles. The naive NRQM provides an explanation of the reduced quark electric multipole being constant, and predicts a linear rise of the reduced spin flip amplitude  $\bar{B}$ , but since  $\bar{C} = 0$ , the NRQM predicts  $m_1^{11} = m_1^{12}$ , in contrast to the experimental findings.

### 3.3 The Transition $\gamma_e + [56, 0^+]_0 \rightarrow [56, 2^+]_2$

The most prominent state of the  $[56, 2^+]_2$  super multiplet is the  $F_{15}(1688)$ . This is the only state in the multiplet that has been studied experimentally over an extended  $Q^2$  range. Similar to the  $D_{13}^+(1520)$ , the photoexcitation dominantly helicity 3/2 and hence  $A_{1/2}^+(F_{15}) \approx 0$ , at  $Q^2 = 0$ . The data show a rapid change in the helicity structure with rising  $Q^2$  (Figure 3.6). The switch to helicity 1/2 dominance is qualitatively reproduced by quark model calculations. Clearly, much improved data are needed for a more definite comparison with the theory.

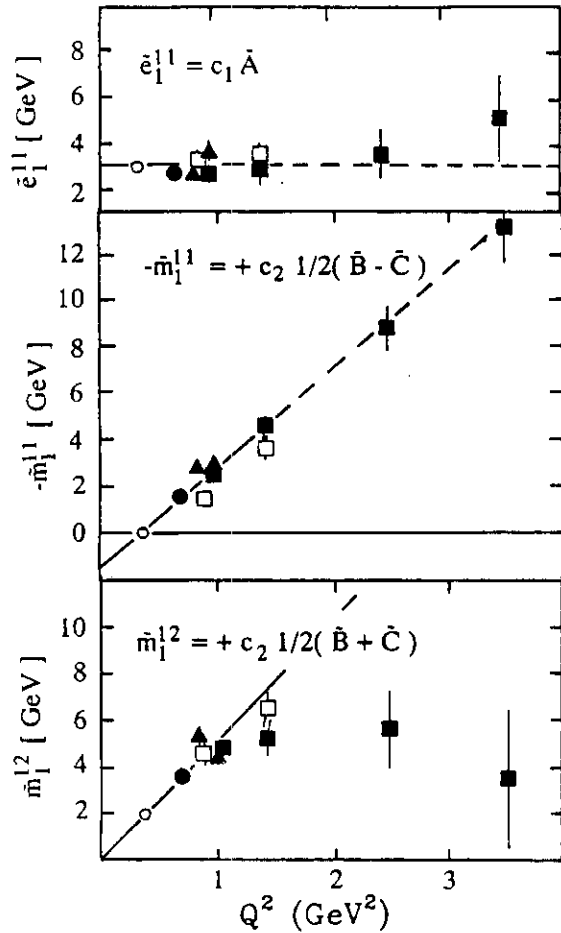


Figure 3.5 Reduced quark multipoles for the transition  $\gamma_\nu + [56, 0^+]_0 \rightarrow [70, 1^-]_1$ . The lines are meant to guide the eye.

A determination of the four contributing SQT amplitudes (note that there is also a spin-orbit flip amplitude D with  $\Delta L_x = 2$ ) is presently not possible because of the lack of electroproduction data for a second state in this multiplet.

### 3.4 Baryon Resonance Transitions at High $Q^2$

At high energies, perturbative QCD makes simple predictions about the asymptotic  $Q^2$  behaviour of the helicity amplitudes for resonance excitation. Based on the theoretical model of Brodsky and Lepage<sup>35</sup>, who factorize the process into a hard scattering part and a

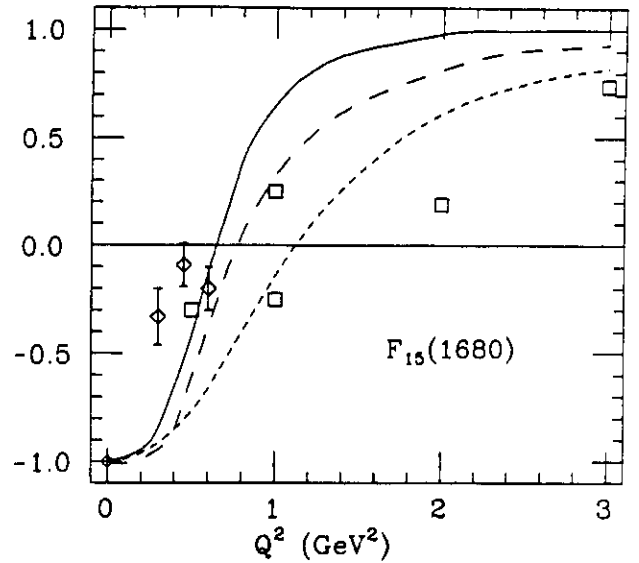


Figure 3.6 Helicity asymmetry for the  $\gamma_\nu p F_{15}(1688)$ . Same models as in Figure 3.3

'soft' non-perturbative part described by quark distribution functions, Carlson<sup>36</sup> has shown that

$$A_{1/2}(Q^2) = C_1/Q^3, \quad A_{3/2}(Q^2) = C_2/Q^5, \quad Q^2 \rightarrow \infty$$

if logarithmic terms are neglected. Information about the quark distribution functions and the normalization constant  $C_1$  can be obtained from QCD sum rules.

Of course, the first question to address is: At what momentum transfer does this description apply? Inclusive data have been interpreted<sup>37</sup> such that this may occur at  $Q^2 \approx 4$  to  $5 \text{ GeV}^2$ . However, others<sup>38</sup> have disputed that claim, arguing that asymptotic behaviour will occur at much higher  $Q^2$ . Conclusive tests require exclusive data, where the resonances are uniquely identified, and their respective helicity amplitudes have been separated. Separated data exist for  $Q^2 \leq 3 \text{ GeV}^2$  only, and only for a few states. In Figure 3.7 the  $A_{1/2}$  data are shown, multiplied by  $Q^3$ . The onset of the asymptotic regime would be indicated by the  $Q^2$  independence of this quantity. This is obviously not the case for this limited  $Q^2$  regime. However, it is interesting to note that the highest  $Q^2$  data are in the ballpark of the asymptotic predictions. It is also interesting to note that for the  $S_{11}(1535)$ , the calculations within the framework of relativized quark models, yield values for the highest  $Q^2$  point which are in the same ballpark as the asymptotic predictions. The non-relativistic version clearly fails for  $Q^2 > 0.6 \text{ GeV}^2$ .

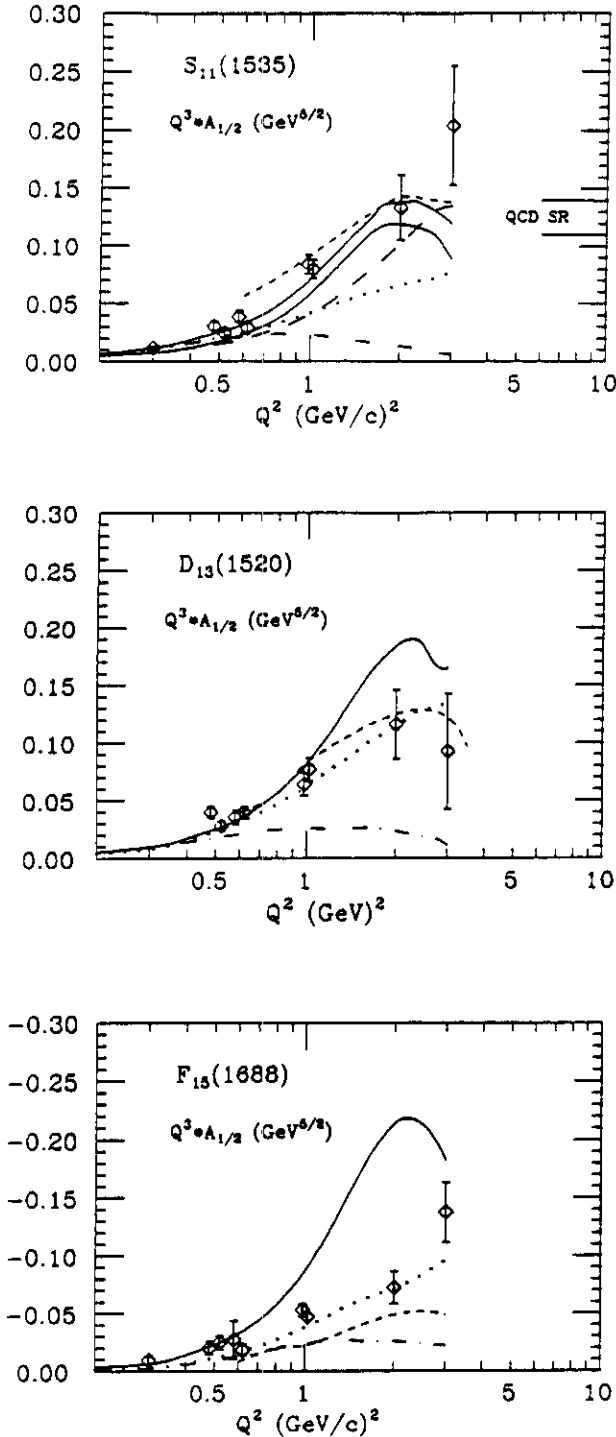


Figure 3.7  $Q^3 A_{1/2}$  for various resonance transitions. Same models as in Figure 3.2. Normalized predictions of Carlson<sup>36</sup> for the asymptotic behaviour of the  $\gamma_p S_{11}$  transition are indicated

#### 4. Experimental Prospects of Electromagnetic Resonance Excitation.

##### 4.1 Single $\pi$ and $\eta$ Production

It is useful to distinguish baryon resonance studies according to the complexity of the final state event. Most of the existing data is single  $\pi$  or  $\eta$  production. This channel is particular sensitive to the lower mass resonances ( $W \leq 1.7\text{GeV}$ ) which decay dominantly into the  $\pi N$  channel, or in the case of the  $S_{11}(1535)$  into  $\eta N$ . Much of the theoretical formalism involved in data analysis has been worked out for these channels. A thorough study of the lower mass region requires precise experimental studies of the single pseudoscalar meson channel. In single pion electroproduction from nucleons 11 independent measurements are needed at a given kinematical point  $Q^2$ ,  $W$ ,  $\theta_\pi$ , to determine the amplitudes of the process  $\gamma_p N \rightarrow N' \pi$  in a model independent fashion. The complete determination of the transition amplitudes in pion and eta production is a long term goal of nucleon resonance physics with electromagnetic probes. This program requires high statistics measurements of unpolarized cross sections, and detailed measurements of polarization observables using polarized beams, polarized nucleon targets, and the measurement of nucleon recoil polarization.

Measurement of the single pion cross section allows determination of four response functions:

$$\frac{d\sigma}{d\Omega} = \sigma_T + \epsilon\sigma_L + \epsilon\sigma_{TT}\cos 2\phi + \sqrt{2\epsilon(1+\epsilon)}\sigma_{TL}\cos\phi$$

Using a polarized electron beam one additional response function can be measured. Measurement of polarization asymmetries with polarized targets or recoil polarimeters will be important. In either case, eight response functions can be measured. Using a polarized beam in conjunction with a polarized target or recoil polarimeter, five more response functions can be accessed. Since polarization observables contain interference terms of amplitudes they are sensitive to small amplitudes and to relative phases between amplitudes. Already, information of limited statistical accuracy will prove extremely sensitive to determining absolute values and signs of small amplitudes which are otherwise not, or only very difficult accessible.

Not all the response functions contain independent information. In particular, only four of the response functions measured with a polarized target are different from the ones measured with recoil polarimeters. In many applications the two methods can be quite competitive, which allows one to select the more convenient techniques.

The main objective is to disentangle the various resonant partial waves. This requires measurement of complete angular distributions with respect to the direction of the virtual photon. Also, measurements in different isospin channels are needed for a separation of resonant and non-resonant amplitudes with different isospin assignments. Complete isospin information can be obtained from a study of the reactions

$$\begin{aligned}\gamma_v + p &\rightarrow p + \pi^0 \\ \gamma_v + p &\rightarrow n + \pi^+ \\ \gamma_v + n &\rightarrow p + \pi^-\end{aligned}$$

In addition, measurement of

$$\gamma_v + p \rightarrow p + \eta$$

selects isospin 1/2, and is a unique means of tagging the  $S_{11}(1535)$  and the  $P_{11}(1710)$  resonances.

The various experimental requirements call for an experimental setup which allows measurement of complete angular distributions in different isospin channels simultaneously.

#### 4.2 Multiple Pion Production.

For higher masses, multiple pion production due to channels like  $\Delta\pi$ ,  $\rho N$ ,  $\omega N$  becomes dominant. Therefore a study of baryon resonance production in this mass region necessitates measurements of these channels. As already mentioned, the QCD motivated extension of conventional quark models predict many states, with masses above 1.8, which have not been observed in  $\pi N \rightarrow \pi N$  reactions. Theoretical calculations<sup>16</sup> indicate that many of the "missing" states tend to decouple from the  $\pi N$  channel due to mixing, however, they may couple strongly to channels like  $\rho N$ ,  $\omega N$ ,  $\Delta\pi$ . Electromagnetic production of these channels may therefore be the only way to have access to these states. In fact, several of these states are predicted to couple strongly to real and virtual photons<sup>39</sup>. For example, the  $F_{15}(1955)$ , and the  $F_{35}(1975)$  should be almost as strongly excited as some of the prominent states at lower masses. Search for these states is important and urgent. Models exist, such as the quark cluster model<sup>40</sup> that can accommodate known baryon states, but predict a fewer number of states.

#### 4.3 Hybrid Baryons States

Recently, there have been speculations about the existence of hybrid baryon states<sup>41</sup> consisting of 3 valence quarks and one valence gluon. The valence gluon gives rise to additional baryonic states (hybrid baryons) ( $Q^3g$ ). In hadronic production experiments these states are difficult to distinguish from ordinary ( $Q^3$ ) states because they are, unlike hybrid mesons, characterized by

quantum numbers which are also possible for the normal baryon states. How can we search for these states using electron or photon beams?

The  $P_{11}(1710)$  has been proposed as a candidate for the lightest hybrid baryons<sup>25</sup>. Others<sup>42</sup> have argued that the mass of the lightest hybrid baryon should not be lighter than 2.2 GeV. In any case, the Barnes-Close selection rule requires

$$A_{1/2}^+(Q^2) \equiv 0, \quad A_{1/2}^0(Q^2) \neq 0$$

for the lightest hybrid  $P_{11}$  state. Hence, it can be photo-produced from neutrons but not from protons. For protons, the experimental photocoupling<sup>43</sup> is consistent with zero within fairly small errors. The neutron data are inconclusive. Measurement of the  $Q^2$  dependence should allow clarification of the nature of this state. A non-zero proton result at any  $Q^2$  would be evidence in favour of the ( $^3Q$ ) nature of the state. The  $Q^2$  dependence can hence be used as a filter to discriminate between ( $^3Q$ ) and ( $^3Qg$ ) states.

#### 4.4 Multiple Quark Transitions

It is well known that the  $[20, 1^+]$  multiplet with its antisymmetric wave function cannot be excited from the ground state in a single quark transition. Experimental evidence for this transition would signal the violation of the SQT hypothesis. Calculations within the framework of a relativized quark model<sup>18</sup> indicate that the MQT amplitudes may be as high as 10 to 20% of those for the SQT process. Clearly, the observation of these transitions requires high statistics measurements under conditions where interferences of the MQT amplitudes with dominant SQT amplitudes are important.

#### 4.5 Experimental Aspects

Many details of baryon resonance excitations, in particular at lower masses, may be addressed with magnetic spectrometers having small solid angles, but being able to withstand high background radiation levels. This way, single pion production in the  $\Delta(1232)$ , or eta production in the  $S_{11}(1535)$  region can be measured with high precision. Small solid angle, high rate magnetic spectrometers may also allow accurate measurements of proton recoil polarizations in reactions such as:

$$\begin{aligned}e + p &\rightarrow e + \bar{p} + \pi^0 \\ e + n &\rightarrow e + \bar{p} + \pi^- \\ e + p &\rightarrow e + \bar{p} + \eta.\end{aligned}$$

Experiments are in preparation at MIT-Bates<sup>44</sup> and at MAMI-B (Mainz)<sup>46</sup>, aimed at precise measurements of

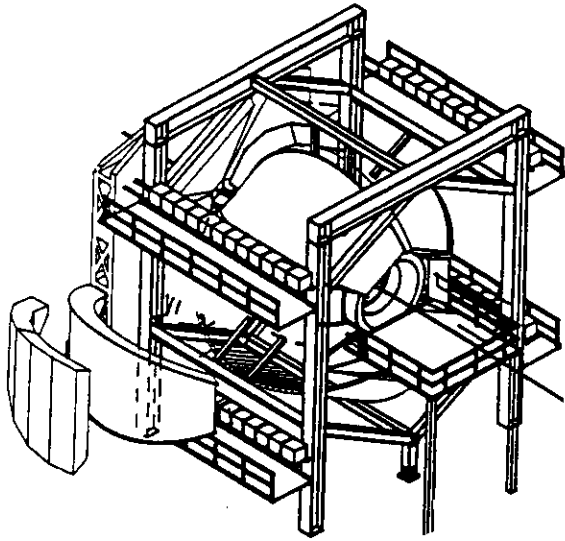


*Figure 4.1 The CEBAF Large Acceptance Spectrometer (CLAS). Six symmetrically arranged superconducting coils generate an approximate toroidal magnetic field. Drift chambers, time-of-flight counters, gas Cerenkov counters, and an electromagnetic calorimeter provide particle identification, charged particle tracking, and energy measurements for electromagnetic particles. The field free region around the target allows use of polarized solid state targets.*

single  $\pi^0$  production off protons in the  $\Delta(1232)$  region, with the goal of extracting more accurate information about the small  $E_{1+}$  and  $S_{1+}$  multipoles.

A comprehensive and efficient experimental program to study electromagnetic transitions of baryon resonances in a large kinematical region, calls for experimental equipment with large solid angle coverage, the possibility to measure neutral particles, and the capability of accommodating polarized proton and neutron targets. At ELSA, the large acceptance spectrometer SAPHIR is nearing completion<sup>46</sup>. This detector is based on a large dipole magnet. It is aimed at measuring multiple pion and kaon photoproduction in the baryons resonance region. At CEBAF, a large acceptance spectrometer (CLAS) based on a toroidal magnetic field has entered the construction phase<sup>47</sup>. A large portion of the scientific program for this detector is aimed at studies of baryon resonance excitations<sup>48</sup> using electron beams. Figure 4.1 shows an artistic view of the CLAS spectrometer.

## 5. CONCLUSIONS

In spite of the enormous effort put into the study of hadronic properties of matter, the field of light quark baryon spectroscopy appears to be still in its infancy. This is due to several factors. First, theoretical guidance based on models which have some relationship to the theory of strong interaction QCD was established only after the bulk of the experiments had been completed. Second, all of the high statistic experiments are single pion production measurements. In view of QCD based quark models, this allows the study of lower mass states with a large elasticity. However, single pion production measurements are not suited for the study of most of the higher mass states. These are predicted to largely decouple from the  $\pi N$  channel, which makes this channel less and less sensitive to resonance excitation in the higher mass region. Third, with the exception of low energy machines such as LAMPF, there are presently no hadron machines available where these experiments could be done in an efficient way. As a consequence, some of the most fundamental problems in intermediate energy, strong interaction physics, the interaction of quarks and gluons in confined systems cannot be addressed experimentally. The only hope is that a machine like KAON in Canada is approved, and that adequate equipment for multi-meson production experiments will be implemented.

The electromagnetic sector suffered from the same shortcomings. In addition, the notorious rate problem in electroproduction experiments prevented high statistics experiments from being carried out, even for single pion production. Fortunately, the prospects in this sector are indeed excellent. With the new CW electron accelerators in the GeV and multi-GeV range now under construction, and with the use of modern experimental equipment, the scientific community will have powerful instruments in hand, which will allow an onslaught on many of the outstanding problems in strong interaction physics.

## 6. ACKNOWLEDGEMENTS

I wish to thank Don Joyce for a careful reading of the manuscript and useful comments. I also want to thank the organizers of the workshop for a very informative time at St. Goar.

## References.

- [1] V. Burkert, Hadron Physics at the New CW Electron Accelerators, these proceedings.
- [2] Particle Data Group, Review of Particle Properties, Phys. Lett. B239 (1990)
- [3] G. Höhler, Nucl. Phys. A508 (1990), 525
- [4] N. Isgur, G. Karl, Phys. Lett. 72B, 109 (1977); Phys. Rev. D23, 817 (1981).
- [5] S. Capstick, N. Isgur, Phys. Rev. D34, 2809 (1986); S. Capstick, Phys. Rev. D36, 2800 (1987)
- [6] D. Menze, Excited Baryons 1988, Troy, NY, 1988, World Scientific Publisher, eds. G. Adams, et al.
- [7] C. Forsyth, R. Cutkosky, Z. Phys. C18, 219 (1983)
- [8] P. Christellin and G. Dillon, Univ. Pisa preprint INPO/TH 88-23 (1988)
- [9] D. Bugg, Phase Locking of Resonances, these proceedings.
- [10] R. Koch, E. Pietarinen, Nucl. Phys. A336, 331 (1980). Höhler, Landolt-Börnstein I/9b2, Springer Verlag (1983)
- [11] R.E. Cutkosky et al., Phys. Rev. D20, 2839 (1979)
- [12] B. Blankleider and G.E. Walker, Phys. Lett. 152B, 291 (1985)
- [13] R.A. Arndt, J.M. Ford and L.D. Roper, Phys. Rev. D32, 1085 (1985)
- [14] R.E. Cutkosky, Proc. 2nd International Workshop on  $\pi N$  Physics (1987), Los Alamos Report, LA-11184-C, pg. 167
- [15] For an overview see: M.E. Sadler, Proc. 2nd International Workshop on  $\pi N$  Physics (1987), Los Alamos Report, LA-11184-C, pg. 200
- [16] R. Koniuk, N. Isgur, Phys. Rev. D21, 1868 (1980)
- [17] D.M. Manley et al., Phys. Rev. D30, 904 (1984) D. M. Manley, Phys. Rev. Lett. 52, 2122 (1984)
- [18] M. Warns et al., Z. Phys. C45, 627 (1990)
- [19] A. Chodos et al., Phys. Rev. D9, 3471 (1974)
- [20] G. Kälberman, J.M. Eisenberg, Phys. Rev. D28, 71 (1988)
- [21] K. Bermuth, D. Drechsel, D. Tiator and J.B. Seaborn, Phys. Rev. D37, 89 (1988)
- [22] G.S. Adkins, C.P. Nappi, Nucl. Phys. B249, 507 (1985)
- [23] A. Wirzba, W. Weise, Phys. Lett. B188, 6 (1987)
- [24] C.E. Carlson, Phys. Rev. D34, 2704 (1986)
- [25] F.E. Close, Proc. Int. Conf. Excited Baryons 1988, Troy, NY, 1988, World Scientific Publisher, eds. G. Adams, et al.
- [26] G. Krösen, B. Boden, CEBAF Report of the Summer Study Group, Newport News, Virginia 23606, RPAC II (1987)
- [27] Z. Li, F. Close, Rutherford Laboratory Preprint RAL-90-010.
- [28] F. Foster, G. Hughes, Z. Phys. C14, 123 (1982)
- [29] W. Konen, H.J. Weber, Univ. of Virginia preprint, UVa-INPP-89-6 (1989)
- [30] C.P. Forsyth, J.B. Babcock, Preprint CMU-HEP 83-4 (1983)
- [31] F.E. Close, F.J. Gilman, Phys. Letts. 38B, 541 (1972); F.E. Close, F.J. Gilman, I. Karliner, Phys. Rev. D6, 2533 (1972)
- [32] A.J.G. Hey, J. Weyers, Phys. Letts. 48B, 69 (1974)
- [33] W.N. Cottingham, I.H. Dunbar, Z. Phys. C2, 41 (1979)
- [34] H. Breuker et al., Z. Phys. C13, 113 (1982). Z. Phys. C17, 121 (1983)
- [35] S.J. Brodsky, G.P. Lepage, Phys. Rev. D24, 2848 (1981).
- [36] C.E. Carlson, J.L. Poor, Phys. Rev. D38, 2758 (1988)
- [37] C.E. Carlson, Proc. 12th Internat. Conf. on Few Body Problems in Physics, Vancouver, July 2-8, 1989.
- [38] N. Isgur and C.H. Llewellyn-Smith, Nucl. Phys. B317, 526 (1989)
- [39] N. Isgur, Proc. CEBAF Summer Workshop 1984, June 25-29, Newport News, Virginia. eds. F. Gross and R. Whitney.
- [40] K.F. Liu, C.W. Wong, Phys. Rev. D28, 170 (1983)
- [41] E. Golowich, E. Haqq, G. Karl, Phys. Rev. D28, 160 (1983); T. Barnes, F.E. Close, Phys. Letts. 123B, 89 (1983).
- [42] N. Isgur and J. Paton, Phys. Rev. D31, 2910 (1985)
- [43] Review of Particle Properties, Rev. Mod. Phys. 56 (1984)
- [44] R. Lourie, V. Burkert (spokesmen), Bates Proposal PR 89-03; C. Papanicolas (spokesman), Bates Proposal PR 87-09.
- [45] G. Adams et al., CEBAF Proposals PR 89-37 - 89-43.
- [46] Reports on Research Activities in Nuclear Physics, 1990 Photonuclear Gordon Conference.
- [47] CEBAF Conceptual Design Report - Basic Experimental Equipment (1990)
- [48] H. Breuker et al., Phys. Letts. 74B, 409 (1978)
- [49] W. Brasse et al., Z. Phys. C22, 33 (1984)
- [50] S. Ono, Nucl. Phys. B107, 522 (1976)
- [51] L.A. Copley, G. Karl, E. Obyrk, Phys. Letts. 29B, 117 (1969)